Completion and performance of the Hobby-Eberly Telescope wide field upgrade

Hill, Gary, Drory, Niv, Good, John, Lee, Hanshin, Vattiat, Brian, et al.

Gary J. Hill, Niv Drory, John M. Good, Hanshin Lee, Brian L. Vattiat, Herman Kriel, Jason Ramsey, Randy Bryant, Jim Fowler, Martin Landriau, Ron Leck, Emily Mrozinski, Stephen Odewahn, Matthew Shetrone, Amy Westfall, Eusebio Terrazas, Edmundo Balderrama, Emily Bevins, Brent Buetow, John Caldwell, George Damm, Phillip MacQueen, Jerry Martin, Amanda Martin, Justin Pautzke, Katie Smither, Sergey Rostopchin, Greg Smith, Renny Spencer, Taft Armandroff, Karl Gebhardt, Lawrence W. Ramsey, "Completion and performance of the Hobby-Eberly Telescope wide field upgrade ," Proc. SPIE 10700, Ground-based and Airborne Telescopes VII, 107000P (6 July 2018); doi: 10.1117/12.2312350

SPIE.

Event: SPIE Astronomical Telescopes + Instrumentation, 2018, Austin, Texas, United States

Completion and performance of the Hobby-Eberly Telescope wide field upgrade*

Gary J. Hill[a†], Niv Drory[a], John M. Good[a], Hanshin Lee[a], Brian L. Vattiat[a], Herman Kriel[a,b], Jason Ramsey[a], Randy Bryant[b], Jim Fowler[b], Martin Landriau[c], Ron Leck[a], Emily Mrozinski[b], Stephen Odewahn[b], Matthew Shetrone[b], Amy Westfall[b], Eusebio Terrazas[b], Edmundo Balderrama[b], Emily Bevins[b], Brent Buetow[b], John Caldwell[b], George Damm[b], Phillip MacQueen[a], Jerry Martin[b], Amanda Martin[b], Justen Pautzke[b], Katie Smither[b], Sergey Rostopchin[b], Greg Smith[b], Renny Spencer[b], Taft Armandroff[a], Karl Gebhardt[a], Lawrence W. Ramsey[d],

[a] McDonald Observatory, University of Texas at Austin, 2515 Speedway, C1402, Austin, TX, 78712-0259, USA

[b] Hobby-Eberly Telescope, 82 Mt. Locke Rd., McDonald Observatory, TX 79734, USA

[c] Lawrence Berkeley National Laboratory, 1 Cyclotron Road Mailstop 50R5008, Berkeley, CA 94720, USA

[d] Pennsylvania State University, 516 Davey Lab, University Park, PA 16802, USA

ABSTRACT

The Hobby-Eberly Telescope (HET) is an innovative large telescope with 10 meter aperture, located in West Texas at the McDonald Observatory. The HET operates with a fixed segmented primary and has a tracker, which moves the four-mirror corrector and prime focus instrument package to track the sidereal and non-sidereal motions of objects. We have completed a major multi-year upgrade of the HET that has substantially increased the field of view to 22 arcminutes by replacing the optical corrector, tracker, and prime focus instrument package and by developing a new telescope control system. The upgrade has replaced all hardware and systems except for the structure, enclosure, and primary mirror. The new, reinvented wide-field HET feeds the revolutionary Visible Integral-field Replicable Unit Spectrograph (VIRUS‡), fed by 35,000 fibers, in support of the Hobby-Eberly Telescope Dark Energy Experiment (HETDEX§), a new low resolution spectrograph (LRS2), the Habitable Zone Planet Finder (HPF), and the upgraded high resolution spectrograph (HRS2). The HET Wide Field Upgrade has now been commissioned and has been in science operations since mid 2016 and in full science operations from mid 2018. This paper reviews and summarizes the upgrade, lessons learned, and the operational performance of the new HET.

Keywords: **Keywords:** Hobby-Eberly Telescope, HET, HETDEX, wide field corrector, tracker, spectrographs: VIRUS, integral field

1. INTRODUCTION

The HET[1-6] (Fig. 1,2) is an innovative telescope designed to be cost-effective for large surveys. It has an 11 m hexagonal-shaped spherical primary mirror made of 91 1-m hexagonal segments that sits at a fixed zenith angle of 35°. HET is the basis for the Southern African Large Telescope (SALT)[7]. It can be moved in azimuth to access about 70% of the sky visible at McDonald Observatory (δ = -10.3° to +71.6°). The pupil was originally 9.2 m in diameter, set by the spherical aberration corrector design, and sweeps over the primary mirror as the x-y tracker follows objects for between

* The Hobby – Eberly Telescope is operated by McDonald Observatory on behalf of the University of Texas at Austin, Pennsylvania State University, Ludwig-Maximillians-Universität München, and Georg-August-Universität, Göttingen

† G.J.H.: E-mail: hill@astro.as.utexas.edu

‡ VIRUS is a joint project of the University of Texas at Austin (UT Austin), Leibniz-Institut für Astrophysik Potsdam (AIP), Texas A&M University (TAMU), Max-Planck-Institut für Extraterrestriche-Physik (MPE), Ludwig-Maximilians-Universität München, Pennsylvania State University, Institut für Astrophysik Göttingen, University of Oxford, Max-Planck-Institut für Astrophysik (MPA), and The University of Tokyo.

§ http://hetdex.org/

Ground-based and Airborne Telescopes VII, edited by Heather K. Marshall, Jason Spyromilio, Proc. of SPIE Vol. 10700, 107000P · © 2018 SPIE
CCC code: 0277-786X/18/$18 · doi: 10.1117/12.2312350

50 minutes (in the south at δ = -10.0°) and 2.8 hours (in the north at δ = +67.2°). The maximum time on target per night is 5 hours and occurs at +63°. The HET primary mirror has a radius of curvature of 26164 mm. The original 4-mirror double-Gregorian type corrector had a 4 arcmin (50 mm) diameter science field of view. Detailed descriptions of the original HET and its commissioning can be found in refs 1-3.

The HET was envisioned originally as a spectroscopic survey telescope, able to efficiently survey objects over wide areas of sky. While the telescope has been very successful at observing large samples of objects such as QSOs and extrasolar planets spread over the sky with surface densities of around one per 10 sq. degrees, the HET design coupled with the limited field of view of the original corrector hampers programs where objects have higher sky densities. In seeking a strong niche for the HET going forward, the HET field of view will be increased from 4′ to 22′ so that it can accommodate the Visible Integral-field Replicable Unit Spectrograph (VIRUS)[8-18], an innovative, highly multiplexed spectrograph that will place 35,000 fibers on sky simultaneously, arranged in 78 fber integral field units (IFUs), and open up the emission-line universe to systematic surveys for the first time, uncovering populations of objects selected by their line emission rather than by their continuum emission properties.

The primary motivation for the HET wide field upgrade (WFU) and VIRUS is to execute the Hobby-Eberly Telescope Dark Energy Experiment (HETDEX[18-19]), which will map the spatial distribution of about 0.8 million Lyα emitting galaxies (LAEs) with redshifts $1.9 < z < 3.5$ over a 420 sq. deg. area (9 Gpc^3) in the north Galactic cap. This dataset will constrain the expansion history of the Universe to 1% and provide significant constraints on the evolution of dark energy. The requirement to survey large areas of sky with VIRUS plus the need to acquire wavefront sensing stars to provide full feedback on the tracker position led us to design an ambitious new corrector employing meter-scale aspheric mirrors and covering a 22-arcmin diameter field of view.

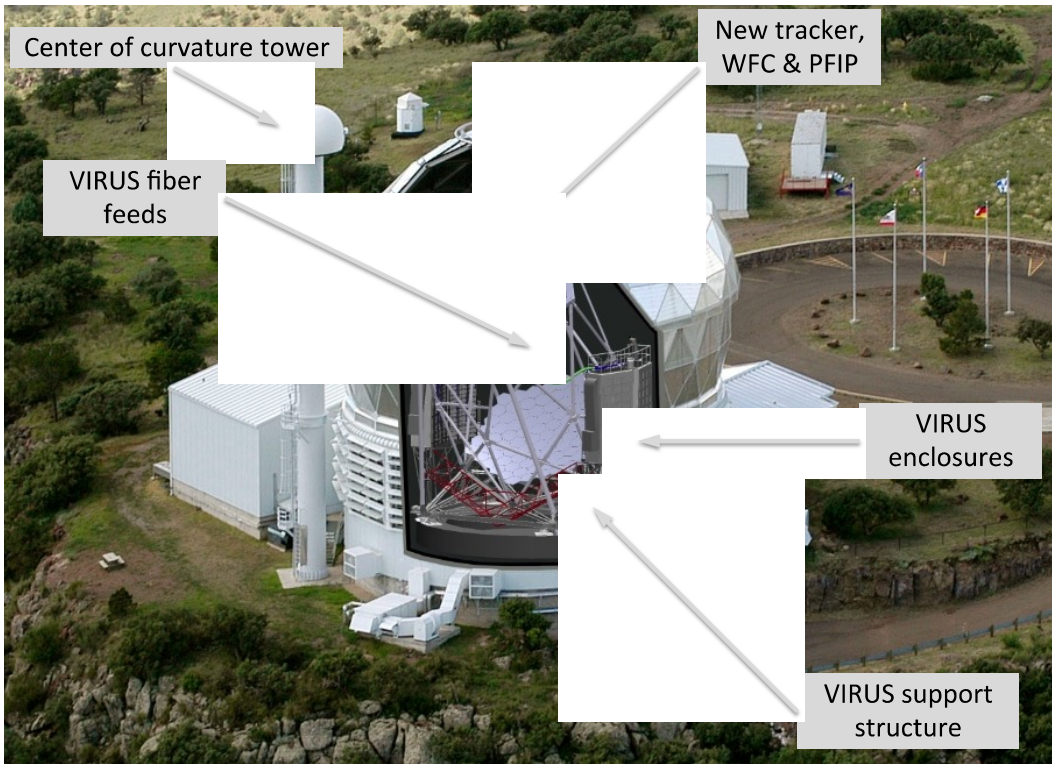

Figure 1. The layout of the HET with rendering of the WFU and VIRUS superimposed. The WFU replaces the top end of the HET with a new tracker, wide field corrector (WFC) and prime focus instrument package (PFIP). The highly replicated VIRUS spectrograph units are housed in two enclosures either side of the structure, which are mounted on the VIRUS support structure, and fed by 35,000 fibers from the prime focus.

The WFU deploys the wide field corrector (WFC[20-24]), a new tracker[25-31], a new prime focus instrument package (PFIP[32-33]), and new metrology systems[34-38]. The metrology systems are intended to provide closed-loop feedback on all axes of motion and the optical configuration of the telescope. They include guiding, wavefront sensing, payload tilt

sensing, and a distance measuring interferometer (DMI). Together they control the alignment of the WFC to the primary mirror as well as providing feedback on the temperature-dependent radius of curvature of the primary mirror, which is on a steel truss.

2. OVERVIEW AND CHRONOLOGY OF THE WIDE FIELD UPGRADE

The basic configuration of the HET is unchanged in the upgrade (Fig. 1), but the new tracker has a much higher payload of 3 tonnes to accommodate the new WFC and PFIP, a five-fold increase. Details of the development of the WFU from conception to installation have been covered in previous proceedings (Refs. 3-6). Here we provide an overview. Table 1 summarizes the timeline of the upgrade from the point at which the original HET was taken off line, after 14 years of science operations.

2.1 Tracker

The new tracker is a third-generation evolution of the trackers for HET and SALT, and is in essence a precision six-axis stage (Fig. 2). The tracker bridge spans the upper hexagon of the telescope structure, moving on two x-axis stages with skew sensing in case they become misaligned. A carriage moves up and down in the y-axis, and supports the hexapod that provides the fine adjustment in the other degrees of freedom. The total volume of motion is about 7x7x4 m^3, and the required accuracy under metrology feedback is on the order of 15 μm and 4 arcseconds in tilt.

Table 1: Chronology of the HET Wide Field Upgrade

Event or Milestone	Date
HET taken off line	Sep-13
New Tracker install	Feb-14
Wide Field Corrector installation	May-15
First Light	**29-Jul-15**
New Low Resolution Spectrograph (LRS2) installed	Nov-15
First 16 VIRUS spectrograph units installed	May-16
Early science operations commence	**Jul-16**
Full queue science operations with LRS2 (2 weeks per month)	Dec-16
Queue science operations transition to 3 weeks per month	Jul-17
Habitable-zone Planet Finder (HPF) delivered	Oct-17
HPF early science operations commence	**May-18**
VIRUS deployment reaches 40 units (half of the total, 18k fibers)	Jun-18
Full science operations commence without engineering periods	**Jun-18**

The tracker was built by the Center for Electro-Mechanics (CEM) and McDonald Observatory (MDO) at the University of Texas at Austin[25-31]. After integration and testing was finished at CEM, we undertook a test plan that was completed in mid 2013[29-31]. Following a Readiness Review in July 2013 for the upgrade, the new tracker was packed and shipped in stages as the original HET tracker was dismantled and the structure prepared for the installation of the new tracker by welding on stiffening sections on the upper and lower beams of the top-hexagon. The upper and lower X-axes were installed in late 2013. The tracker bridge was the last major item to be shipped and installed over 2 days in February 2014. The hexapod actuators were manufactured by ADS International (Valmadrera, Italy) in collaboration with CEM and MDO[26]. The hexapod system was installed and the tracker commissioned in mid 2014. The tracker motion control system (TMCS) is based in the Matlab-Simulink environment in a dSPACE controller[39]. The Telescope Control System (TCS[40,41]) handles all the high-level functions and most of the coordinate transforms and mount models for the tracker. The TMCS environment limits the ability to perform complex calculations on the 2.5 ms update rate, so TCS interprets all the higher-level functions for the TMCS and receives status updates 5 times per second. Development of the TMCS at CEM lagged significantly and necessitated MDO personnel taking over responsibility for the system.

While at CEM, we mapped the deflections of the new HET tracker as a first step in creating the mount model for the telescope. We utilized a laser tracker and SMR retro-reflectors, to measure the deflections of the tracker subsystem, using a dummy WFC to mimic the load. These measurements created a transform with low-order terms and a saddle shape. Once mounted at HET, this mapping process was repeated and the tracker deflections re-derived in reference to the structure and primary mirror (Sec. 3.2).

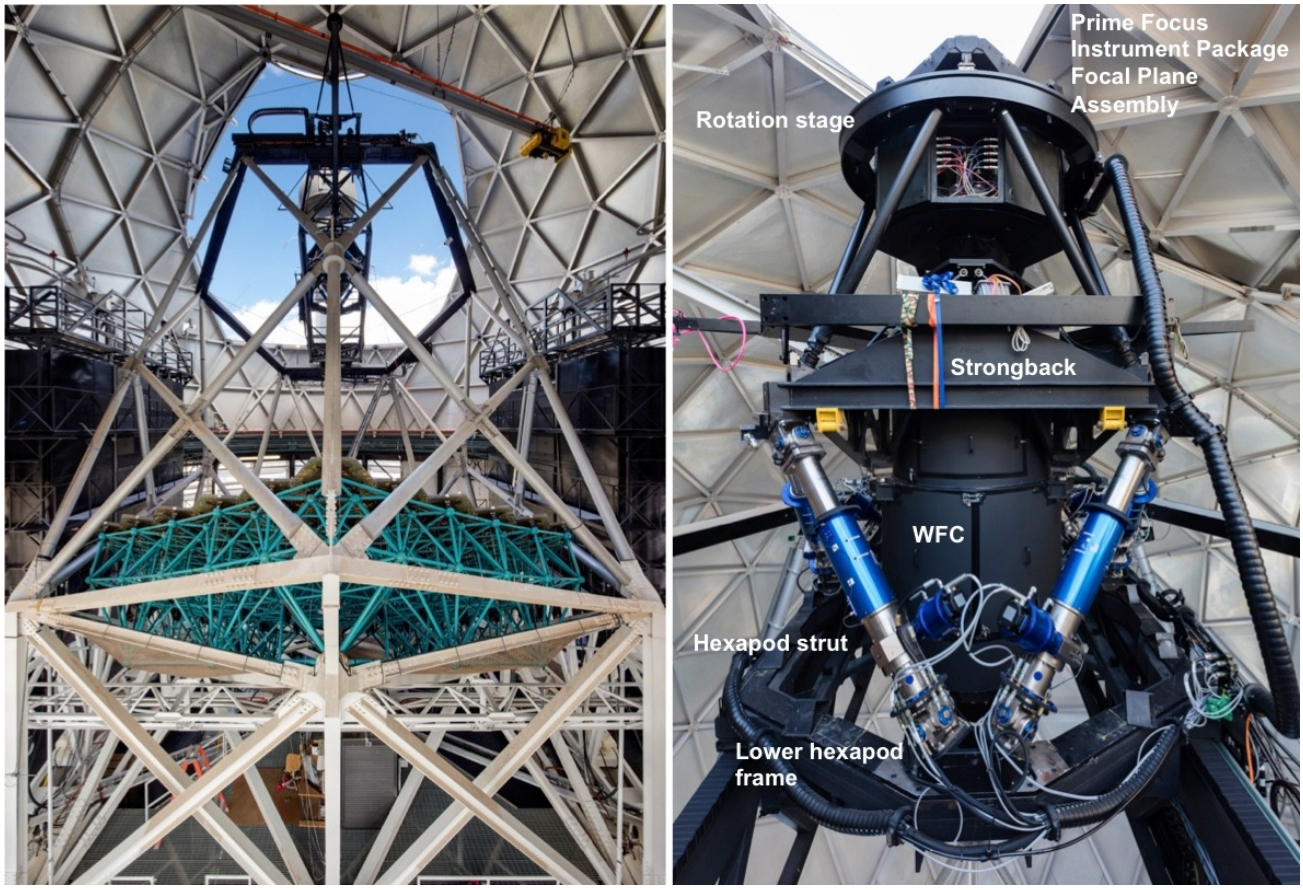

Figure 2: Images of completed HET upgrade. Left – view from behind primary mirror, showing the new tracker centered in the upper hexagon of the telescope structure, and showing the VIRUS enclosures either side of the telescope. Right – view of the WFC and PFIP with key components indicated. The hexapod struts that orient the WFC to the primary mirror can be identified by their blue casings. The focal plane assembly (FPA, at the top of the structure) is supported by a fixed hexapod for alignment and a rotational stage that keeps the orientation on sky during a track.

2.2 Wide Field Corrector (WFC)

The new corrector (Fig. 3) has improved image quality compared to the previous corrector, a 22 arcminute diameter field of view and a 10 m pupil diameter. The periphery of the field is used for guiding and wavefront sensing to provide the necessary feedback to keep the telescope correctly aligned. The WFC is a four-mirror design with two concave one meter diameter mirrors, one concave 0.9 meter diameter mirror, and one convex 0.23 m diameter mirror. The corrector is designed for feeding optical fibers at f/3.65 to minimize focal ratio degradation, and so the chief ray from all field angles is normal to the focal surface. This is achieved with a concave spherical focal surface centered on the exit pupil. The primary mirror spherical aberration and the off-axis aberrations in the wide field are controllable due to the first two mirrors being near pupils, and the second two mirrors being well separated from pupils to control field aberrations. The imaging performance is 0.6 arcsec or better over the entire field of view, and vignetting is minimized. The WFC was manufactured by the University of Arizona College of Optical Sciences (OSC)[20-22]. Figuring and polishing of the three large mirrors was done at OSC on robotic swing-arm machines and tested with swing-arm profilometry using non-contact sensors. The degree of aspheric departure and the steepness of the surfaces of the large mirrors proved a challenge. Testing of the large mirrors used a combination of non-contact swing-arm profilometry, tied to laser tracker measures of the radius of curvature, and interferometric confirmation of figures using phase-etched computer generated holograms (CGHs). Testing was completed in March 2013. As part of the figure test, centering fixtures were aligned that were intended to be used in the final alignment of the WFC assembly. These center fixtures have CGH targets that provide a reference that locates the center and normal of each mirror surface. The smaller M4 was subcontracted to Precision Asphere, and utilized a transmission test with CGH.

Reflective coatings for the WFC[22,23] are required to have high reflectance (95% or better from 350 nm 1800 nm), and are challenging, being based on silver and multiple dielectric layers. Experience with coating degradation on the old HET corrector led us to adopt a sealed design for the WFC with entrance and exit windows and careful sealing of the WFC housing. Since deployment, the WFC has been purged with nitrogen gas. The facility has a large volume of nitrogen available from the cooling system for VIRUS, and this is utilized to provide an over-pressurized oxidation-free environment for the mirror coatings to achieve the longest life possible. The large mirrors were coated by JDSU and M4 was coated by Zecoat. M4 sees a very wide range of incident angles, and required a more complex coating than the others. MDO designed and constructed the complex fixturing needed to safely support the large mirrors during cleaning and coating at JDSU[23].

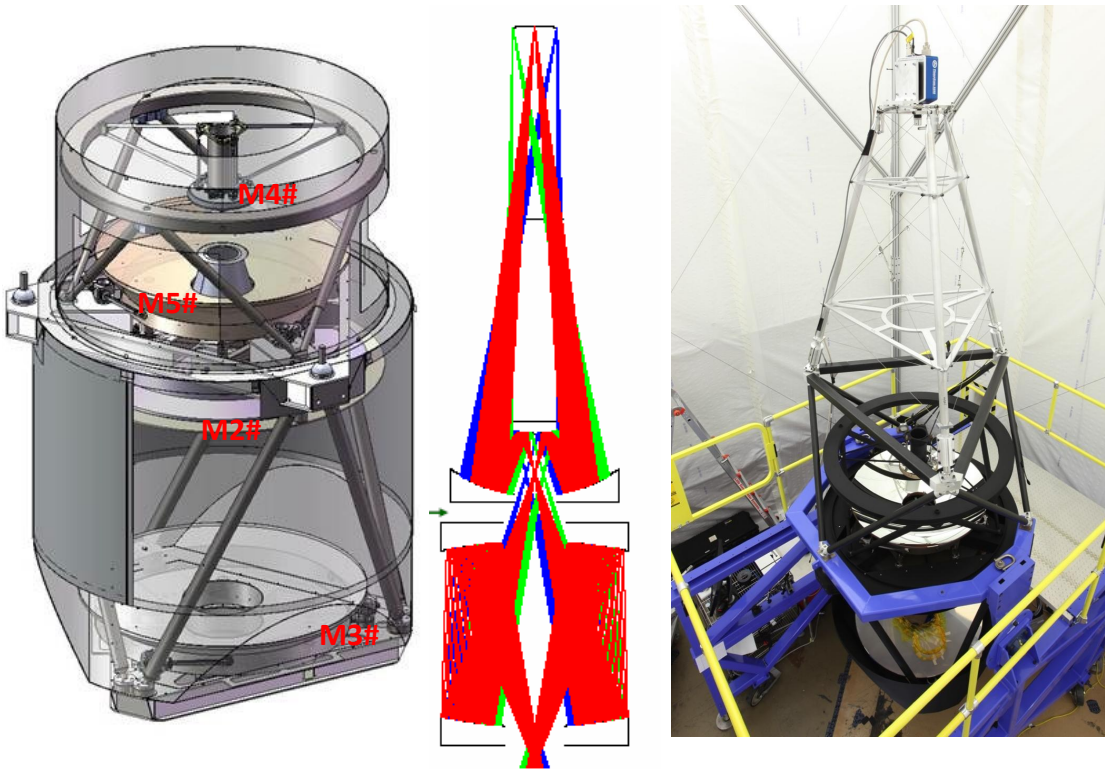

Figure 3. Layout of WFC mirrors and structure (left), optical layout (center), and WFC alignment at UA OSC (right). Image credits H. Lee and UA OSC.

The alignment scheme developed by UA OSC relied on the center references to locate the mirror surfaces using a combination of an interferometer and autocollimator to set centration and tilts and a LT to set separations. Then interferometric CGH tests of the M4/M5 pair the M2/3 pair and of the whole system were to be used to evaluate the alignment of the assembly. A number of problems were uncovered once he WFC was assembled and alignment started[22]. Errors in figuring of M3 and M5 were detected and led to a redesign of the mirror separations and the addition of an aspheric corrector plate (manufactured by Asphericon), in place of the exit window. With these changes the WFC design could meet specifications. Drift of the centering fixtures led to loss of the tilt reference that necessitated a change of plan for the final alignment. Following diagnosis of this problem, an alternative alignment scheme utilizing the M2/3 and M4/5 subsystem interferometric CGH pair tests was developed to align in tilt. The center references were sufficient for centration and separation. In addition, MDO developed a conjugate test for M4/5 utilizing a Shack-Hartmann wavefront sensor that allowed for some off-axis information to be gathered[22] and break degeneracies with the remaining full-system on-axis interferometric system test. The results were analyzed and reviewed, with the conclusion that there was some residual misalignment uncovered by the conjugate test, manifesting in a possible tilt of the focal surface that could place the WFC performance outside acceptable bounds. The issue was that, in order to keep the position angle fixed on sky during a track, the physical focal surface must rotate relative to the fixed WFC, so a tilted optical surface could not be aligned simply by tilting the focal plane assembly to match. However, the majority of realizations of the state of the

WFC allowed by the conjugate test data resulted in tilts well within specification with only two that placed it outside specification. Following external review of the results, it was agreed that the WFC likely would meet specifications and the only way to gain further information was to integrate it with the HET primary mirror and perform on-sky testing to verify the system.

The WFC was transported (very carefully and at night) to HET on May 28, 2015[6,22,24]. Following a repeat of the interferometric system test inside the HET facility, to verify that there had been no movement of mirrors during transportation, we installed the WFC on HET on July 2, 2015, followed by the PFIP, which was aligned to the WFC optical axis using a laser tracker and an alignment telescope, referenced to a target at the center of the Input Head Mount Plate (IHMP, see below) that defines the physical focal surface. Alignment of the WFC to M1 was achieved by direct measurement with an alignment telescope hung under the WFC and aligned to the center reference on M4 in the WFC that defines its optical axis. The alignment telescope was then reversed in its mount to point at the center segment of M1 and the tracker was moved to align (in X,Y, and tip/tilt) with cross hairs strung across that segment, by introducing offsets in the tracker position. These offsets were small (on the order of 20 mm, indicating the accuracy of the tracker setup) and defined the center of the track from an optical perspective. Reversing the alignment telescope again to look out of the dome at the Center of Curvature Alignment System (CCAS) tower, we verified that the optical axis of the telescope was aligned very closely to the entrance aperture of the CCAS alignment instrument that defines the center of curvature of the primary mirror. This confirmed that the axis is aligned with the primary mirror center of curvature as defined by the source in the Mirror Alignment Recovery System (MARS[43]) in the center of curvature tower, which is used to stack the mirror segments to a common center of curvature at the start of each night. We had completed a dry-run of this alignment procedure using a dummy corrector, while we waited for the WFC to be completed, so this procedure was completed in a few days and we achieved first light on July 29th 2015, immediately achieving good pointing within an arcminute, and excellent image quality on the acquisition camera (1.3 arcsec FWHM, consistent with the expected median image quality of the system).

Achieving good on-axis image quality at first light did not vindicate the alignment of the WFC, however, due to the residual uncertainties discussed above, so over the Fall of 2015 we undertook on-sky tests with miniature wavefront sensors deployed over the field of view (mounted in the VIRUS IFU seats in the input head mount plate (IHMP), see below) as a final confirmation of the performance of the WFC. By this point we were able to track both sidereal objects and geostationary satellites (GS) with high reliability. Testing of the WFC alignment required us to set up a GS on each of the dWFS in turn, measuring the wavefront as a function of field position. Details of these tests and analysis are provided in Ref. 22. We detected only a small tilt of the optical focal surface relative to the IHMP, within specifications, and could eliminate the possible scenarios that would have failed our requirements.

2.3 Prime Focus Instrument Package (PFIP) and metrology systems

The PFIP[32,33] rides on the tracker and consists of several subassemblies (Figs. 2,4). The WFC mounts on a strongback on a three ball-in-vee kinematic mount. The strongback mounts to the tracker hexapod and the structure of PFIP is built up around the corrector. The focal plane assembly (FPA), shown in Fig. 4, contains all the hardware at the focus of the telescope including the acquisition and guiding (AG) assembly, fiber instrument feeds, a large rotary shutter, and electronics hardware. At the focal surface there is the input head mount plate (IHMP) that is a precision-machined interface for the VIRUS IFUs and other fiber feeds. It defines the physical focal surface and mounts to the dither mechanism that makes the precision dither offsets needed to fill in the fiber pattern of the VIRUS IFUs. A strain relief guides the IFU conduits to both sides of the tracker. A set of temperature controlled, insulated enclosures house electronics hardware and the FCU input sources, optics, and selection mechanisms. The pupil plane assembly (PPA) is located in between the wide field corrector and the focal plane assembly. It contains a stationary and moving set of baffles at the exit pupil of the telescope and a platform for the aspheric corrector plate and eventually an atmospheric dispersion compensator (ADC) for the wide field corrector. The deployment of the PPA has been split into phases. Initially, the support structure with fixed exit pupil baffle and the corrector plate have been deployed. The next phase will see the moving baffle deployed. The Lower Instrument Package (LIP) is mounted to the input end of the wide field corrector, and provides a seal. The LIP is a platform for the entrance window changer, tip-tilt camera, and facility calibration unit (FCU) output head. The FCU illuminates the pupil and focal surface of HET with a pattern that quite closely mimics that obtained on sky[43].

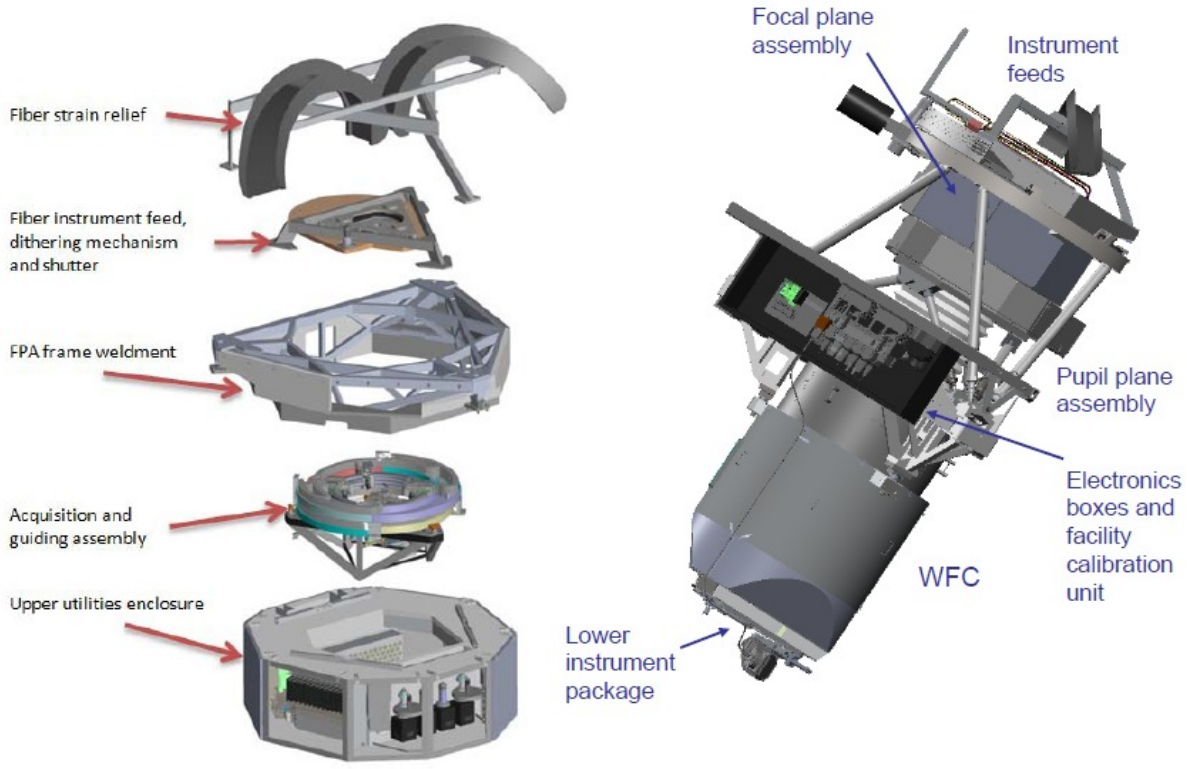

Figure 4. Renderings of the Prime Focus Instrument Package (PFIP). On the right the full assembly is shown with major sub-assemblies indicated. On the left is an exploded view of the FPA showing its major components. The FPA contains most of the complexity of the instrument, including the acquisition and guiding (AG) assembly with guide probes and wavefront sensors.

HET requires constant monitoring and updating of the position of its components in order to deliver good images. The WFC must be positioned to 15 μm precision in focus and X, Y, and 4.0 arcsec in tip/tilt with respect to the optical axis of the primary mirror. This axis changes constantly as the telescope tracks, following the sidereal motions of the stars. Tilts of the WFC cause comatic images. In addition, the global radius of curvature (GROC) of the primary mirror can change with temperature (as it is essentially a glass veneer on a steel truss), and needs to be monitored. The segment alignment maintenance system (SAMS[44]) maintains the positions of the 91 mirrors with respect to each other, but is less sensitive to the global radius of curvature of the surface. The feedback to maintain these alignments requires excellent metrology, which is provided by the following subsystems:

- Guide probes to monitor the position on the sky, and plate scale of the optical system, and monitor the image quality and atmospheric transparency
- Wavefront sensors (WFS) to monitor the focus and tilt of the WFC
- Distance measuring interferometer (DMI) to maintain the physical distance between the WFC and primary mirror
- Tip-tilt sensor (TTS) to monitor the tip/tilt of the WFC with respect to the optical axis of the primary mirror

The upgrade adds wavefront sensing[34-38] to HET in order to close the control loop on all axes of the system, in conjunction with the DMI adapted from the current tracker metrology system and a new TTS[32]. There is redundancy built into the new metrology system in order to obtain the highest reliability. Two guide probes distributed around the periphery of the field of view provide feedback on position, rotation, and plate scale, as well as providing a record of image quality and transparency as a function of wavelength. The alignment of the corrector is monitored by the wavefront sensors as well as by the DMI and TTS. The radius of curvature of the primary mirror is monitored by the combination of focus position from the WFS with the physical measurement from the DMI and checked by the plate scale measured from the positions of guide stars on the guide probes. The SAMS edge-sensors provide a less sensitive but redundant feedback on radius of curvature as well.

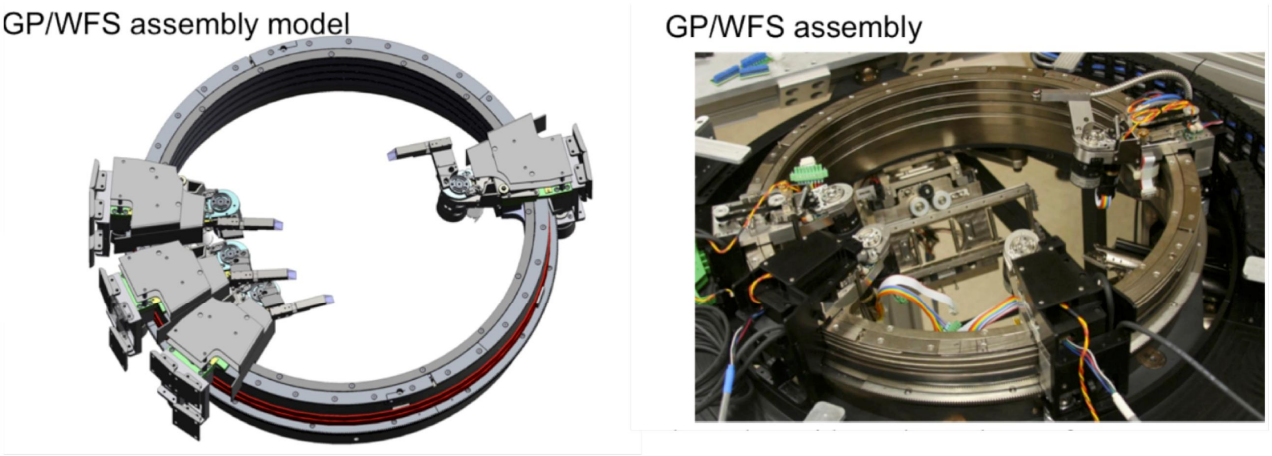

Figure 5. Rendering of the guideprobe assembly (left) and the assembled unit undergoing testing in the lab prior to deployment (right). Four swing arms position two guideprobes and two wavefront sensors in the outer 3 arcminute radial annulus of the HET field (credit B. Vattiat).

The heart of the metrology system for the WFU is the AG assembly[32,33] (Fig. 5), which mounts the guide probe assembly, the acquisition camera, a wavefront sensor and a pupil viewer. The light is directed to these by deployable pickoff mirrors with pneumatic actuators. The guide probe assembly is used for star guiding of the telescope, wavefront sensing feedback to the telescope focus, and observing conditions (image size, transparency, and sky brightness). There are four probes; two imaging probes and two wave-front sensing probes.

The two guide probes use small pick-off mirrors and coherent imaging fiber bundles to select guide stars from the outer annulus of the field of view. They are located ahead of the focal surface, before the shutter. Each ranges around the focal surface on precision encoded stages, accessing a 180 degree sector. They are designed to have a small size to reduce shadowing of the focal surface, and each has a field of view of 22.6 arcsec on a side.

Two Shack-Hartmann (S-H) wavefront sensors also range in the outer field. Their function is to provide feedback on the low-order errors in the wavefront (focus, coma, spherical, and astigmatism)[34,37]. These errors are caused by misalignment of the corrector with the primary mirror focal surface and by global radius of curvature and astigmatism errors in the primary mirror shape. Updates will be generated approximately once per minute. In addition to the WFS probes there is an analysis wavefront sensor, selectable within the FPA by deploying a pickoff mirror, that allows more detailed feedback analysis of the image quality. It was used extensively as the reference for telescope focus during the commissioning phase and is available for long-term monitoring of the system focus over time. The design of the wavefront sensors is straightforward, but their application to the HET, with the varying illumination of the telescope pupil during a track, requires development of a robust software system for analysis of the sensor data to produce reliable wavefront information.

Fig. 6 shows examples of the varying pupil illumination of HET during a track[37]. In order to derive accurate wavefront measurements from the S-H sensors, an accurate model of the illumination was required. This is illustrated in Fig. 6 along with an example of a WFS image. Images are obtained typically on a 5 second cadence and the two WFS provide redundant information that can be checked for consistency. The WFS focus and tip/tilt errors are used to correct the DMI and TTS zero points, respectively. When the DMI correction reaches a threshold the radius of curvature of the primary mirror SAMS system is adjusted by the telescope operator at the next convenient time (specifically not done during an observation since the primary mirror takes a number of cycles to settle after such a correction).

PFIP was deployed on HET in July 2015. It is a very complicated instrument in its own right, and has been commissioned in phases from July 2015 to May 2016. The commissioning procedure established frames of reference for the various cameras (Acquisition Camera, Guide Probes and Wavefront Sensors) within the higher-level control software. The AG assembly requires a mount model that was measured with a laser tracker in the lab prior to shipment and verified on sky. The guide and WFS field rotate with the swing of the arms and the azimuth position of their carriages. The analytic model transforming the field positions and rotations onto sky was refined using accurate astrometry from the integral field VIRUS instrument.

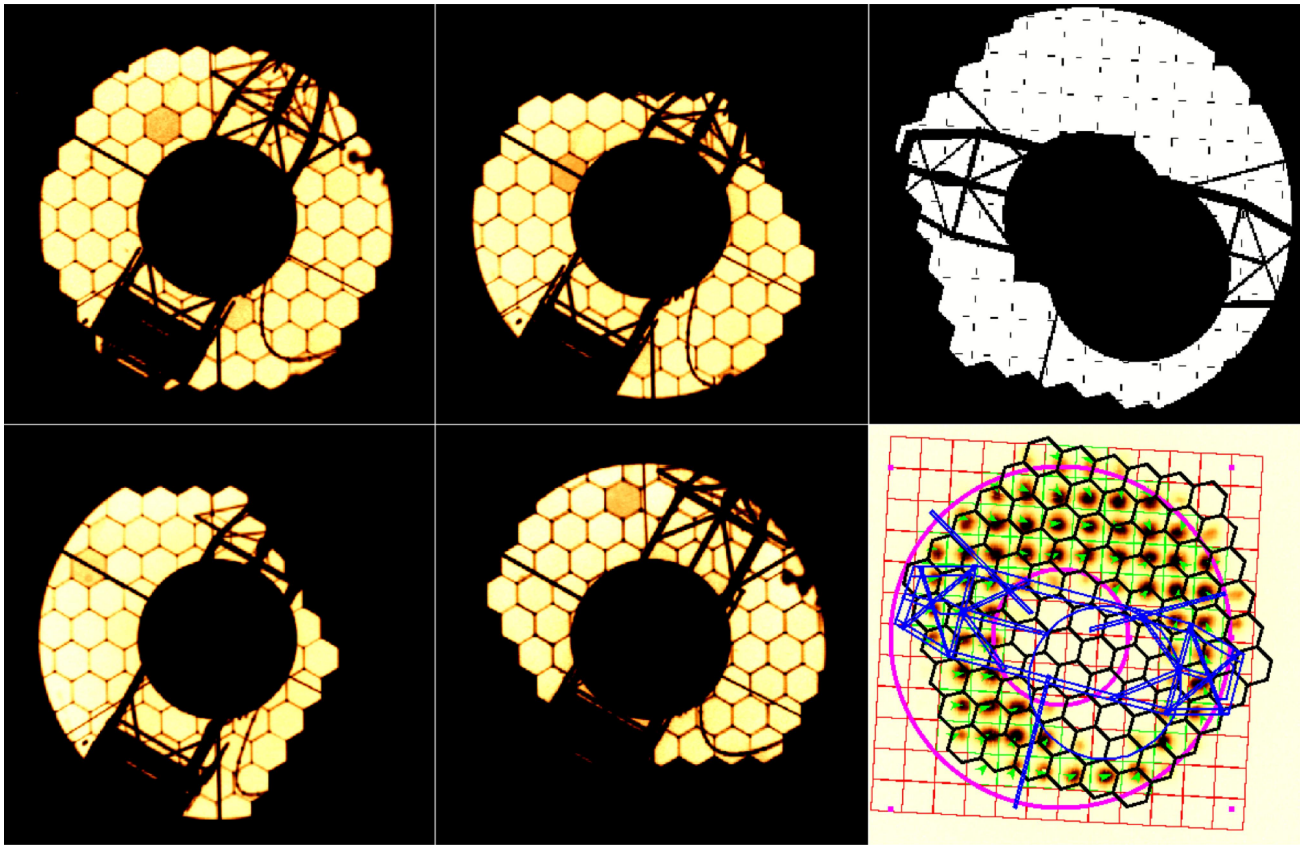

Figure 6. Examples of the variations in pupil illumination of the HET. The left four images show views from the Pupil Viewer camera. The work platform obstructing light in the lower left of each image has subsequently been removed. The top right image shows the pupil illumination model that incorporates the obstructions of the WFC and the tracker bridge, as well as the pupil position on the primary mirror. Bottom right is a WFS image with illumination features overlaid (credit H. Lee). See text for details.

3. TELESCOPE CONTROL SOFTWARE & MOUNT MODEL DEVELOPMENT

The performance of the HET is completely dependent on metrology and the control software system, since the telescope is about to go out of alignment at any moment. The WFU has tight specifications on pointing, tracking and guiding performance (in all axes) that have been met by a combination of careful systems design and detailed analysis of performance referring to physical models of the hardware.

3.1 Telescope control System

The new integrated software control system for the HET WFU is described in Refs. 40,41. It uses a component architecture providing a high degree of monitoring, automation, scriptability and scalability. It consists of a network of control systems, each of which models a sub-set of closely coupled hardware. The control systems (CS) communicate with each other using simple but flexible messaging scheme encoding commands to subsystems and events informing of state changes. Each system is responsible for specific functions based on type or proximity to hardware, and is designed to be run autonomously. For engineering purposes, each subsystem can also be scripted independently of others. The primary systems for the WFU and VIRUS are the Telescope CS (TCS), the Prime Focus Instrument Package CS (PFIP-CS), the Payload Alignment CS (PAS), the VIRUS Data Acquisition CS (VDAS), and the Tracker motion CS (TMCS), along with a centralized logging system. In addition to these control systems, GUI interfaces for the telescope operator and resident astronomer have been developed. The TCS is responsible for coordinating the operation of all other CS and knowledge of the high-level astronomy-related state is restricted to TCS. PFIP-CS controls the hardware on PFIP, while the PAS is responsible for gathering metrology from various alignment systems, including the guiders, WFS, TTS, and the DMI needed to close all tracker-motion related loops. Logging from TMCS is at 5 Hz and from other subsystems at

their native update rates. The logger is failsafe, logging into local databases if the central log-server is down. These local databases are synchronized automatically with the central log server when it is available. In addition to log messages, logging can be configured to log any subset of events generated by the system, to obtain very detailed execution traces. This is done without interfering with the operation of the CS generating no additional overhead or changes in timing. The primary operating system is Red Hat Enterprise Linux 6.x, 64-bit. The software was developed with an agile process using the standard GNU toolchain, and widely available libraries. The TCS has been controlling the telescope since delivery of the tracker and is now a mature system. The software for VDAS (called CAMRA) controls VIRUS units and LRS2[45].

3.2 Mount models

The original HET system utilized a heuristic mount model based on on-sky measurements, which convolved the many physical effects that contribute to the pointing and tracking accuracy of the integrated system. Adjustments to improve pointing would often result in poorer tracking accuracy, and vice-versa.

For the WFU, we set out to base the mount model on direct physical measurement of subsystems that could be combined to create a deterministic correction to the tracker position with well-understood physical underpinnings. Our primary tool in this was laser tracker and SMR retro-reflectors, which we utilized to understand the deflections of the tracker subsystem, using a dummy WFC to mimic the load. These measurements were tied to the telescope frame and reference points on the primary mirror to create a transform with low-order terms that accounted for the deflections of the tracker relative to the ideal tracking sphere. These measurements were further refined using the TTCAM and DMI to provide direct measurements of the payload relative to the surface of M1, and thereby tie the tracker frame to the optical frame provided by the primary mirror, aligned by the center of curvature CCAS instrument.

As described in Sec. 2.2, the optical axis of the WFC, with the IHMP centered and normal to the optical axis, provided the reference for the tracker payload. It was aligned normal to the center segment of the primary mirror by adjusting tracker position, using a video alignment telescope (VAT). The VAT was then flipped to view the CCAS instrument aperture, which defines the center of curvature of the primary mirror. The alignment was very close and when we went on sky this reference system placed us within an arcminute of the intended pointing.

After a period of evaluation, we found that there was a small rotational error for tracks in the north. The rotation stage at the top of the PFIP compensates for the field rotation as HET tracks. This error was on the order of an arcsecond across the field (~0.1 deg error) and was traced to an error in the hexapod transform implemented by CEM, which chose the solution that allows the hexapod platform to rotate. Since this error was fixed, we have achieved excellent tracking at all declinations, without any need to actively guide in the rotation axis. This case highlights the benefit of seeking a physical model for errors that might otherwise be corrected by an ad-hoc mathematical correction. The model has much higher accuracy than any model that is based on pointing and tracking corrections, and in addition improvements in pointing lead to improvements in tracking and vice-versa, the opposite of our experience with the first realization of the HET.

The telescope structure sits on 4 feet on a very flat concrete pier. Deflections of the telescope structure during the track, due to the unbalanced loading as the payload moves in X,Y, were also measured against the telescope pier and incorporated as a further layer of mount model terms that transform the tracker frame to the projection on sky. As the telescope is moved in azimuth to access different declinations there is also a term in the pointing mount model that accounts for the non-flatness of the pier. A key recent insight is that the telescope rocks on the 4-point mount so that we need separate mount models for the east and west tracks. There is also evidence that this aspect of the mount model may be seasonal, perhaps because the polypropylene pads on the feet vary in stiffness with temperature. This possibility is being investigated, but the current mount model meets the quite stringent pointing requirements needed for efficient observing with VIRUS (see below).

This physical approach to the mount model has proven very successful with pointing residuals now meeting requirements and goals over the whole tracker range. Just as important, drift rates are very low and correlate closely with pointing residuals, which bears out the expectation that improvements in one will be reflected in the other.

4. SCIENCE INSTRUMENTATION

The new instrument suite for the upgraded HET emphasizes the telescope's strengths in large surveys and synoptic time-domain spectroscopy. All the new instrumentation is fiber-fed so as to exploit the azimuthal scrambling inherent to fiber transmission, and the WFC is designed to be telecentric to feed fibers. This scrambling is particularly important for a telescope like HET with a variable pupil illumination. There are two low resolution fiber integral field instruments (VIRUS[10] and LRS2[45], described in more detail below) and two fiber-fed high resolution instruments (HPF[46,47] and HRS2[48,49]) that reside in the basement spectrograph room inside the telescope pier.

The Habitable-Zone Planet Finder is a highly temperature stabilized, fiber-fed, NIR high resolution spectrometer, built from the ground up to be capable of discovering low mass planets around mid-late M dwarfs. It has been developed by Pennsylvania State University. The optical design of the HPF is an asymmetric white pupil spectrograph layout in a vacuum cryostat cooled to 180 K. The spectrograph uses gold-coated mirrors, a mosaic echelle grating, and a single Teledyne Hawaii-2RG (H2RG) NIR detector with a 1.7-micron cutoff covering parts of the information-rich z, Y and J NIR bands at a spectral resolution of R~55,000. The use of 1.7 micron H2RG enables HPF to operate warmer than most other cryogenic instruments. Precision wavelength calibration is based on a laser comb. The HPF fiber feed can be seen mounted in the IHMP, near the center of the HET field in Fig. 7.

The upgraded High Resolution Spectrograph (HRS2) is based on the original HRS[48], which was in operation for over a decade, and is being upgraded to work with image slicing and volume phase holographic grating cross dispersers to improve efficiency, and reformatted to allow a future blue arm to be added. It is being developed by McDonald Observatory.

At the time of writing LRS2 is in full science operation, half the VIRUS units are deployed and HPF is in shared-risk science observing.

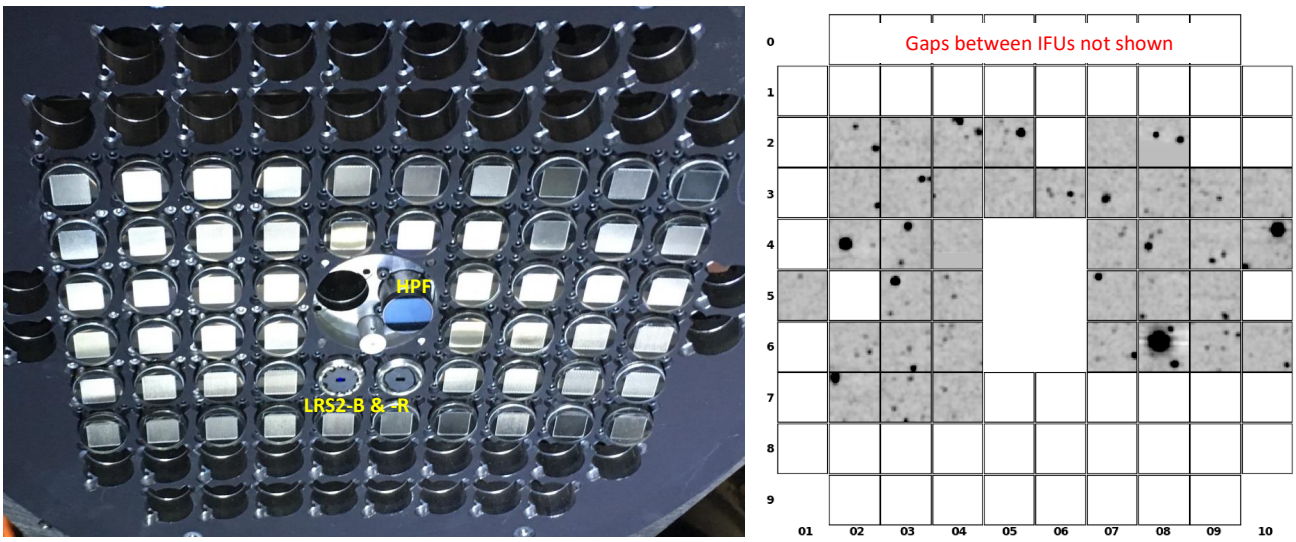

Figure 7: Left – photon's-eye view of the deployed IFUs for LRS2 and VIRUS mounted in the precision input head mount plate (IHMP), along with the fiber feed for the HPF high resolution spectrograph (credit E. Mrozinski). LRS2 has two small full-fill IFUs mounted close to the central mounting boss for the high resolution spectrographs, where the fiber feed for HPF is mounted. The other central hole is for the future HRS2 high resolution spectrograph. The LRS2-B and LRS2-R IFUs are 100 arcsec. apart on the sky, which is the same pitch as for the VIRUS IFUs. 54 VIRUS IFUs are installed, currently. Each covers 50x50 sq. arcsec. For scale, the corner VIRUS IFUs in this image are ~18 arcminutes apart, which is ~190 mm. Right – example of data from VIRUS on a typical HETDEX field with 39 spectrograph units deployed (credit K. Gebhardt). The spectral dimension is collapsed to create images for each IFU, and this representation does not show the gaps between the IFUs.

4.1 VIRUS

VIRUS[8-18] consists of 156 identical spectrographs (arrayed as 78 pairs, each with a pair of spectrographs) fed by 35,000 fibers, each 1.5 arcsec diameter (1.8 arcsec^2), on sky. VIRUS has a fixed bandpass of 350-550 nm and resolving power R~750. The fibers are grouped into 78 integral field units (IFUs), each with 448 fibers and 20 m average length. The 448 fibers at the input of each IFU are arrayed in a 1/3 fill-factor hexagonal pattern such that a set of three dithered exposures will fill in the 50 x 50 arcsec^2 area. The 78 IFUs are arranged in a grid pattern covering approximately a 16 arcminute diameter field with a fill-factor of 1/4.5 and obtain blind spectroscopy of 60 sq. arcminutes of sky area per observation.

The motivation for VIRUS is the Hobby-Eberly Telescope Dark Energy Experiment (HETDEX[6,13]), which will map the spatial distribution of about 0.8 million Lyα emitting galaxies (LAEs) with redshifts $1.9 < z < 3.5$ over a 420 sq. deg. area (9 Gpc^3) in the north Galactic cap and an equatorial field. This dataset will constrain the expansion history of the Universe to 1% and provide significant constraints on the evolution of dark energy. The advantage of an integral field spectrograph for this project is that the tracer galaxies are identified and have their redshifts determined in one observation.

VIRUS spectrographs have been developed by the University of Texas at Austin McDonald Observatory and Texas A & M University, the IFUs have been led by the Leibniz Institute for Astrophysics (AIP), and many parts have been supplied by Oxford University. Data reduction software has been developed by the Max-Planck-Institut für Extraterrestriche-Physik (MPE) and UT Austin. VIRUS is the first example of large-scale replication applied to optical astronomy and is capable of surveying large areas of sky, spectrally. The replication model offers significant cost-savings on components and engineering when compared to traditional monolithic astronomical instruments. The full VIRUS array will simultaneously observe 35,000 spectra with 14 million resolution elements. In total, VIRUS has 0.7 Gpixels, comparable to the largest imagers yet deployed.

The VIRUS array has been undergoing staged deployment starting in late 2015. Figure 7 shows 54 VIRUS IFUs deployed in the IHMP at the focus of HET, along with the IFUs of LRS2 and the HPF fiber feed. At the time of writing, 40 of the VIRUS IFUs are attached to spectrograph units and the right panel of Fig. 7 shows the projection on sky of a field observed as part of the HETDEX survey which started in started in 2017 December.

VIRUS will be used to survey 450 sq. degrees (100 sq. degrees observed) with blind spectroscopy for HETDEX. This dataset will be unique and will have many applications beyond constraining the evolution of dark energy. The prospect of serendipitous discoveries is exciting with this new wide field blind spectroscopic observing mode being opened up.

4.2 LRS2

The second generation Low Resolution Spectrograph (LRS2[45]) is a four-channel integral field spectrograph that is based on an adaptation of the VIRUS unit design. As a result, we were able to develop the instrument quickly and the spectrograph units benefit from utilizing the VIRUS support infrastructure (see below). It replaces the original LRS[50] that was an imaging spectrograph and not compatible with the WFU. Designed as a powerful small-object spectroscopic follow-up platform, LRS2 is based on the design of VIRUS and provides integral field spectroscopy for two seeing-limited fields of 6″×12″ with unity fill factor. It offers increased resolving power, broader wavelength coverage and higher throughput than the original LRS.

The replicable design of the VIRUS spectrograph units was leveraged for LRS2 to gain broad wavelength coverage from 370 nm to 1.05 μm, spread between two fiber-fed dual-channel spectrographs that operate in unison but observe independent fields that are separated by 100″. The location of the two IFU inputs can be seen in Fig. X. Volume phase holographic grism dispersers allow higher resolving power than the VIRUS units. The blue spectrograph pair, LRS2-B, covers $364 \leq \lambda\ (\text{nm}) \leq 467$ and $454 \leq \lambda\ (\text{nm}) \leq 700$ at fixed resolving powers of $R = \lambda/\delta\lambda \approx 2500$ and 1400, respectively, while the red spectrograph pair, LRS2-R, covers $643 \leq \lambda\ (\text{nm}) \leq 845$ and $823 \leq \lambda\ (\text{nm}) \leq 1056$ with both of its channels having $R \approx 2500$. The integral field units each incorporate a unique dichroic beamsplitter at their inputs to divide the light between the two channels of the spectrograph units.

The two LRS2 spectrograph units were deployed at HET between November 2015 and February 2016. They entered early science operations in July 2016. As with the original LRS which was a workhorse instrument on the original HET, LRS2 is being used for a wide range of science from targets of opportunity (e.g. Supernovae) to extremely faint high redshift targets such as radio galaxies and Lyman-break galaxies.

4.3 VIRUS and LRS2 Support Infrastructure

VIRUS and LRS2 are fiber-fed which allows the mass of the spectrographs to be carried in two enclosures, one on each side of the telescope (Figs. 1,8). Each enclosure can support 40 pairs of spectrographs, there is capacity for the 78 VIRUS units and the two units of LRS2. The VIRUS support infrastructure, installation, and maintenance procedures are described in Ref. 16.

The key configuration change to the facility is the addition of the enclosures and support structure for VIRUS. The final VIRUS enclosure locations were a compromise that was strongly influenced by the need to maintain man-lift access to the primary mirror. Since the wavelength coverage of VIRUS extends down to 350 nm, the average fiber length had to be minimized commensurate with keeping the mass of the instrument off the telescope structure and providing sufficient access to the primary mirror and tracker with the HET man-lifts and crane. Following extensive optimization and evaluation by HET staff, we settled on a configuration with VIRUS units housed in two large enclosures flanking the telescope structure and riding on a separate air-bearing system during rotation of the telescope in azimuth (Fig. 1). The VIRUS Support Structure (VSS)[27] is a complex weldment that interleaves with the main telescope structure without applying loads to it that could couple wind induced vibration from the enclosures to the telescope. It rides on separate air-bearings that lift it during changes in telescope azimuth, and is pulled round by the main azimuth drive. The enclosures are large clean rooms with air circulation and heat extraction to remove heat from the VIRUS controllers and ensure that the skin temperature of the enclosures remains close to ambient to ensure they do not impact the dome seeing. The weldments for the enclosures were procured by MDO and were outfitted with hatches, seals, cables and the heat removal system by TAMU[13].

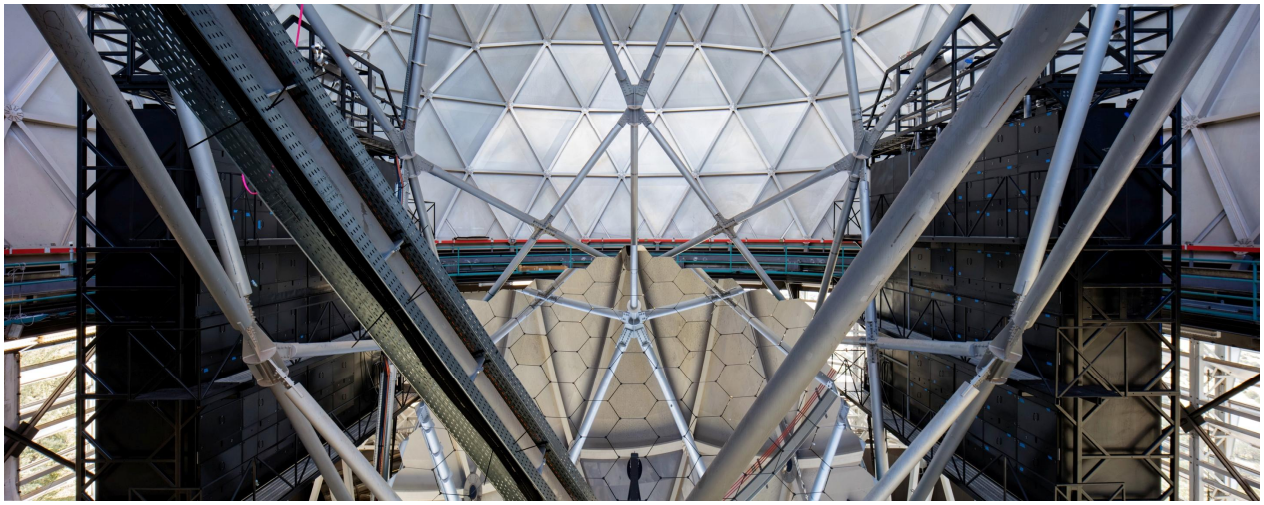

Figure 8: View of the HET from the front showing the primary mirror and the large VIRUS enclosures either side of the telescope structure. They sit on the VIRUS support structure (VSS), which moves on air bearings to follow the azimuth setting of the telescope. The phase separator tanks of the VIRUS Cryogenic System (VCS) can be seen mounted to the top of each enclosure.

The distributed and large-scale layout of the VIRUS array presented a significant challenge for the cryogenic design[14-16]. Allowing 5 W heat load for each detector, with all losses accounted for and a 50% margin, the cooling source is required to deliver 3,600W of cooling power. We engaged George Mulholand of Applied Cryogenics Technology to evaluate the options and provide an initial design. Following a trade-off between cryocoolers, small pulse-tubes and liquid nitrogen based systems, it was clear that from a reliability and cost point of view liquid nitrogen is the best choice[14,15]. The problem of distributing the coolant to the distributed suite of spectrographs is overcome with a gravity siphon system fed by a large external LN tank. A trade-off between in-situ generation of the LN in an on-site liquefaction plant, and delivery by tanker has been made, with the result that the delivery option is both cheaper and more reliable.

An important aspect of the cryogenic design is the requirement to be able to remove a camera cryostat from the system for service, without impacting the other units. This is particularly difficult in a liquid distribution system. A design was developed that combines a standard flexible stainless steel vacuum jacketed line (SuperFlex) to a cryogenic

bayonet incorporating copper thermal connector contacts into each side of the bayonet. When the bayonet halves are brought together they close the thermal contact. The resulting system is completely closed, i.e., it is externally dry with no liquid nitrogen exposure. The camera end of the connector is connected by a copper cold finger to the detector. This design has another desirable feature: in normal operation the SuperFlex tube slopes downwards and the bayonet is oriented vertically. Liquid evaporation will flow monotonically up in order to avoid a vapor lock. If the bayonet is unscrewed and raised upwards, a vapor lock will occur and the bayonet will be cut off from the cooling capacity of the liquid nitrogen. This effectively acts as a "gravity switch", which passively turns off cooling to that camera position.

The VIRUS Cryogenic System (VCS) was constructed by Midwest Cryogenics[9]. The 11,000 gallon vacuum jacketed tank was installed by Praxair in October 2014. The enclosures were delivered to HET and the VCS installed in Nov 2014 and Feb 2015. The system was first turned on in Feb 2015 and now operates continuously cooling more than 40 spectrograph units distributed in both enclosures. A 6,000 gallon delivery of LN is be required every two to three weeks. Praxair is making regular deliveries triggered by metrology on the main tank that indicates LN level.

An essential part of VCS is its safety system. This system continuously monitors critical variables (e.g. dome atmosphere oxygen levels, LN pressure, LN flow rates, and LN storage tank levels). When predefined set points are exceeded the system automatically activates strategically located audio and visual alarms, and if required closes the main LN supply line valve. Each afternoon the system undertakes an auto-test of the alert system, and sends test telephone alerts to the recipient list. This ensures that the system cannot go off-line for an extended period without being noticed.

Table 2: Performance requirements for HET upgrade compared to performance of the old HET and current performance of the HET WFU. Except for setup times for HETDEX, performance is meeting or exceeding all requirements and most goals.

Performance area	Requirement	"old" HET	Upgraded HET	Comment
Pupil diameter	10 m class	9.2 m	**10.0 m**	At center of track
Field of view	22 arcmin diameter	4 arcmin	**22 arcmin**	70 times larger area at same level of field vignetting
Median on-axis image quality EE(50%)	1.25 arcsec EE(50%)	1.7 arcsec	**1.3 arcsec**	In median 1.0 arcsec site seeing
Open-loop pointing (rms)	25 arcsec (goal 9 arcsec)	30 arcsec	**90% < 12 arcsec absolute**	This level now achieved over full tracker range
Setup time (end of exposure to start of next)	< 5 minutes 90% of the time	10-20 mins	**4-7 minutes (<5 min 50% of time)**	Upgrade can set up blind on invisible targets in same time
HETDEX setup time	5 min w/ Az move, 1.5 min no move	-	**5 min w/ Az move, 4.1 min no move**	with OCD observing automation; 1.5 min for no Az move is a goal
Setup accuracy (rms)	0.25 arcsec (0.1 arcsec goal)	0.5 arcsec	**0.2 arcsec**	Ability to center target on fiber, slit, or IFU; measured on old LRS and new LRS2
Metrology System	full sensing of all degrees of freedom	only guiding	**All degrees**	Wavefront sensing feedback completes all degrees of freedom, particularly focus
Guiding residuals	0.25 arcsec rms	0.5 arcsec	**0.10 arcsec rms**	including field rotation and plate scale
focus tracking	15 um rms	200 um	**17 um rms**	under wavefront sensor (WFS) control
tip/tilt residuals	10 arcsec rms	30 arcsec	**2 arcsec rms**	Tip/tilt tracked by both TTS and WFS

5. CURRENT PERFORMANCE OF HET AND REMAINING WORK

The HET WFU is now complete with the telescope resuming full science operations. Table 2 summarizes the performance compared to the requirements and goals of the WFU along with a comparison to the metrics for the old HET. All the metrology subsystems are working as intended and we have found the control loops of the tracker to be extremely robust due to the tracker hardware design[31]. More recently, we have focused on the mount model and on improving operational efficiency, spending typically a week per month in engineering, centered on full moon since we did not until recently have a bright-time instrument deployed.

As an example of performance, Figure 9 shows an examples of guiding and wavefront sensing during a full 1.5-hour track in the north. The left panel shows the centroids of guide images demonstrating <0.1 arcsec. rms. The top right hand panel of Fig. 9 shows the performance of a wavefront sensor detecting focus and tip/tilt of the WFC. Note the rapid

correction at the start of the track followed by corrections to focus of +/-20 microns and tip/tilt of +/- 5 arcseconds. The lower right hand panel shows the variation of image quality measured from one of the guiders over a track, indicating good image quality at the edge of the field. This serves to demonstrate that the image quality from the optics meets requirements over the full field. The delivered image size of the HET is still dominated by errors of the primary mirror (stack and segment figures) and by dome seeing in cold seasons. The wavefront sensor output also allows higher Zernike terms of the image quality to be studied and the image of each S-H subaperture is a measure of seeing in an aperture of about one-meter scale. We are using the several million WFS images obtained in the past two years to study seasonal variations in delivered image quality. The TCS and its subsystems log a huge number of events that we monitor and are beginning to utilize for performance investigations, such as this. See Refs. 37,38 for details.

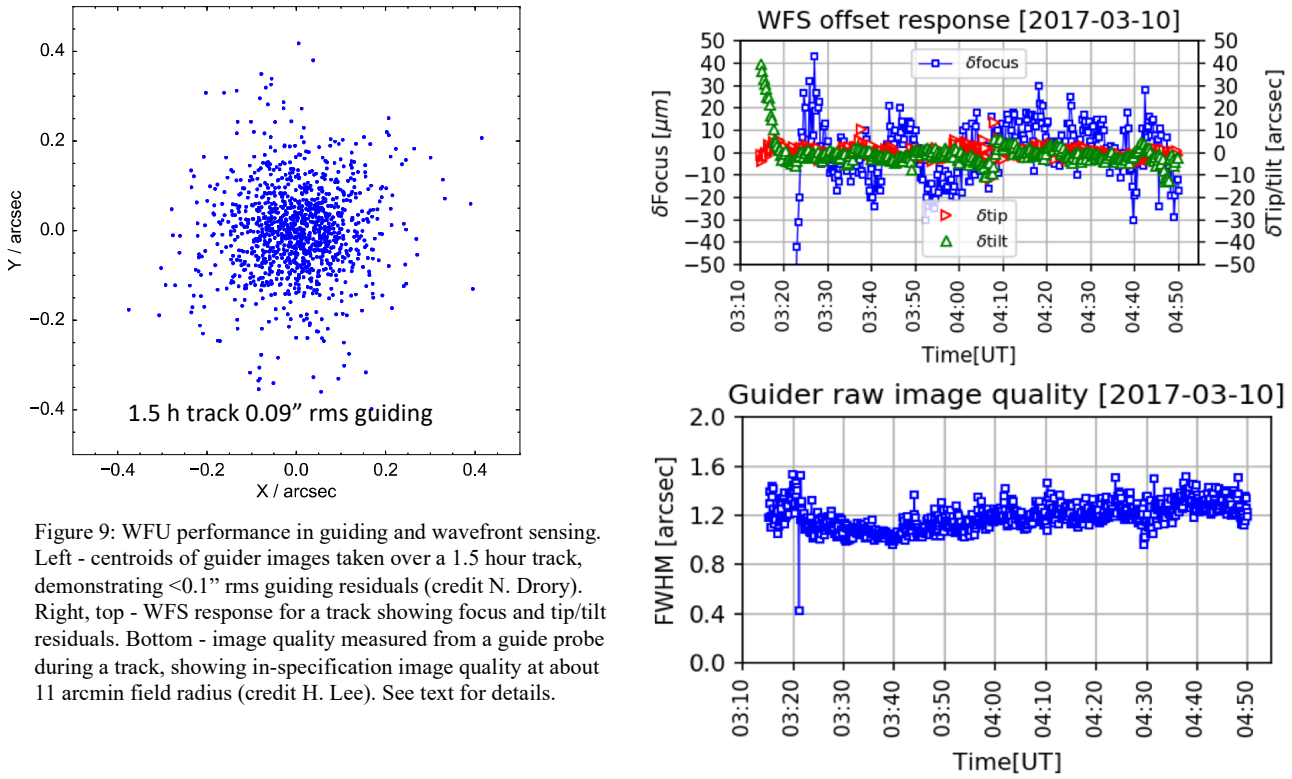

Figure 9: WFU performance in guiding and wavefront sensing. Left - centroids of guider images taken over a 1.5 hour track, demonstrating <0.1” rms guiding residuals (credit N. Drory). Right, top - WFS response for a track showing focus and tip/tilt residuals. Bottom - image quality measured from a guide probe during a track, showing in-specification image quality at about 11 arcmin field radius (credit H. Lee). See text for details.

Telescope pointing and tracking have been improved as described in Sec. 3.2. With the physical mount model improvements in pointing are also reflected in improved tracking. A key requirement for efficient observing with VIRUS is that we be able to point the telescope such that most observations start with the guiderstars within the 22 arcsec. GP fields. This is now achieved 90% of the time, and allows setup to be achieved simply by centering the guidestar without the overhead needed to deploy the acquisition camera. Fig. 10 shows the improvements in pointing over the first part of 2018 and the

The ability to orchestrate the telescope control system has also led to improvements in efficiency. The Observing Conditions Decision (OCD) tool is a Python state machine that monitors the event stream from the metrology system to decide whether observing conditions are suitable for HETDEX observing. When they are, OCD selects the best field and (if allowed) will automatically slew the telescope and perform the observation with only a minimal setup step needed from the Telescope Operator. This orchestration has improved operational efficiency for HETDEX observing with VIRUS (Fig 10, left) and is accomplished within a framework that will allow other instruments to interact with the telescope. The framework is also being used by HPF. While setup overheads have been driven down quite significantly during 2018, and meet requirements, we have not achieved the aggressive goal of achieving 1.5 minute setups for VIRUS observing when no azimuth change is required. Detailed examination of the events stream from the TCS will led to further improvements (the extrapolation in Fig 10 represents modest improvements in areas we can already identify). The consequence of missing the goal is a 7% increase in the 2200 hours of observing projected to complete HETDEX.

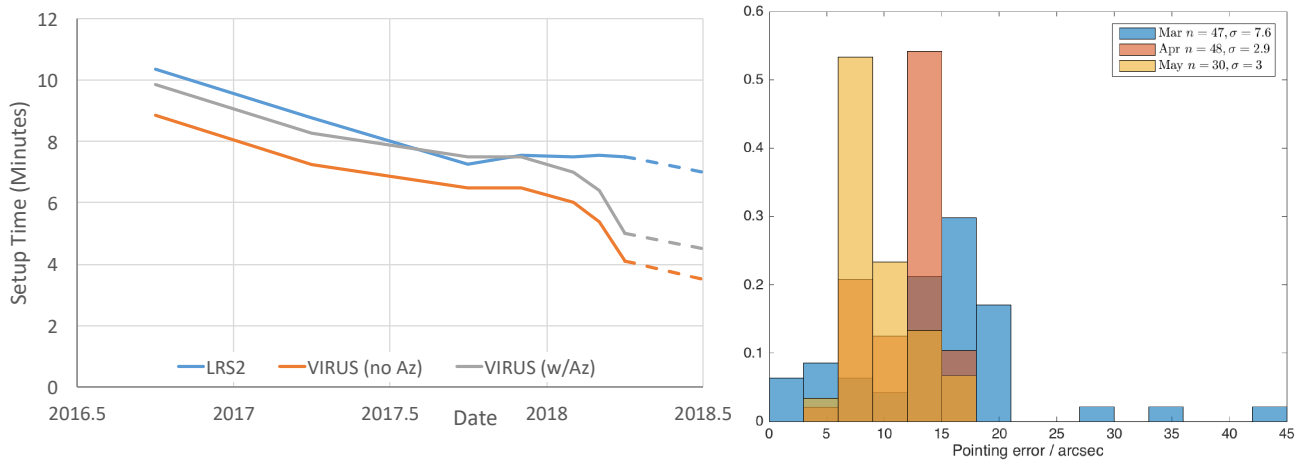

Figure 10: Performance metrics for the HET WFU. Left – setup time in minutes for LRS2 and VIRUS (with and without a change in azimuth) as a function of time. Setup time is defined as the time from the shutter close on the previous observation to the next shutter open command. There has been a steady increase in operational efficiency and recently significant improvement in the setup times for VIRUS due to improved pointing and the use of OCD to automate observing (See text for details). Dashed lines represent expected improvements, though the timeframe is uncertain. Right – histograms of frequency against pointing error demonstrating pointing improvements between March (blue) and May (yellow) 2018.

In parallel with the WFU installation, the primary mirror segments are being recoated with a dense Aluminum reflective coating in a new coating facility on site. At this time, all segments will have been cycled through the facility and the average age is below 12 months. Recoating and cleaning with dry ice snow is an ongoing effort to maintain the primary mirror reflectivity in the best possible state.

6. SUMMARY

HET was taken off line at the end of August 2013. The removal of the old spherical aberration corrector, PFIP, and tracker followed by the installation of the new tracker was complete in May 2014. A year later the WFC was delivered from UA OSC, and first light was achieved in July 2015. Testing of the system and refinement of the software and mount-models demonstrated that the WFU has achieved its goals. Instrument installation and commissioning started in November 2015 and the new HET entered early science operations with the new Low Resolution Spectrograph (LRS2) on July 1, 2016. Since then, the performance of the HET has been refined and now meets all requirements and most goals. The infrared high resolution spectrograph Habitable-zone Planet Finder (HPF) was installed in October 2017 and is now in shared risk science operations. The upgraded high-resolution spectrograph (HRS2) will be deployed later. Full science operations for the upgraded HET commenced in June 2018.

ACKNOWLEDGEMENTS

HETDEX (including the WFU of the HET) is run by the University of Texas at Austin McDonald Observatory and Department of Astronomy with participation from the Ludwig-Maximilians-Universität München, Max-Planck-Institut für Extraterrestriche-Physik (MPE), Leibniz-Institut für Astrophysik Potsdam (AIP), Texas A&M University (TAMU), Pennsylvania State University, Institut für Astrophysik Göttingen, University of Oxford and Max-Planck-Institut für Astrophysik (MPA). In addition to Institutional support, HETDEX is funded by the National Science Foundation (grant AST-0926815), the State of Texas, the US Air Force (AFRL FA9451-04-2-0355), by the Texas Norman Hackerman Advanced Research Program under grants 003658-0005-2006 and 003658-0295-2007, and by generous support from private individuals and foundations.

We thank the following reviewers for their valuable input at various stages in the project:

- Science Requirements Review 6-26-07, Roland Bacon, Gary Bernstein, Gerry Gilmore, Rocky Kolb, Steve Rawlings

- Preliminary Design Review 4-10-08, Bruce Bigelow, Gary Chanan, Richard Kurz, Adrian Russell, Ray Sharples
- PFIP Integration and Alignment Review 7-26-11, Larry Ramsey, Bruce Bigelow, Steve Smee, Mike Smith
- Tracker Factory Acceptance Test Plan Review 3-8-11, Povilas Palunas, Jeffrey Kingsley, Dave Chaney
- Wide Field Upgrade Readiness Review, 7-16-13, Daniel Fabricant, Fred Hearty
- Wide Field Corrector Pre-shipment Review 4-22-15, Daniel Fabricant, Fred Hearty
- VIRUS Detector System Review, 2-1-16, Roger Smith, Ian McLean, Phillip MacQueen

We thank the staffs of McDonald Observatory, the Hobby-Eberly Telescope, and the Center for Electromechanics, University of Texas at Austin, the University of Arizona College of Optical Sciences, and Department of Physics and Astronomy, TAMU, for their contributions to the HET Wide Field Upgrade.

REFERENCES

[1] Booth, J.A., Wolf, M.J., Fowler, J.R., Adams, M.T., Good, J.M., Kelton, P.W. Barker, E.S., Palunas, P., Bash, F.N., Ramsey, L.W., Hill, G.J., MacQueen, P.J., Cornell, M.E., Robinson, E.L., "The Hobby-Eberly Telescope Completion Project", in *Large Ground-Based Telescopes*, Proc SPIE 4837, 919 (2003)

[2] Hill, G.J., MacQueen, P.J., Shetrone, M.D., & Booth, J.A., "Present and future instrumentation for the Hobby-Eberly Telescope", Proc. SPIE, 6269-5 (2006)

[3] Hill, G.J., MacQueen, P.J., Palunas, P., Barnes, S.I., Shetrone, M.D., "Present and future instrumentation for the Hobby-Eberly Telescope", Proc. SPIE, 7014-5 (2008)

[4] Hill, G.J., *et al*., "Current status of the Hobby-Eberly Telescope wide field upgrade," *Proc. SPIE*, 8444-19 (2012)

[5] Hill, G.J., Drory, N., Good, J., Lee, H., Vattiat, B.L., Kriel, H., Bryant, R., Elliot, L., Landiau, M., Leck, R., Perry, D., Ramsey, J., Savage, R., Damm, G., Fowler, J., Gebhardt, K., MacQueen, P.J., Martin, J., Ramsey, L.W., Shetrone, M., Schroeder, E., Cornell, M.E., Booth, J.A., and Moriera, W., "Deployment of the Hobby-Eberly Telescope Wide Field Upgrade", Proc. SPIE, 9145-5 (2014)

[6] Hill, G.J., Drory, N., Good, J.M., Lee, H., Vattiat, B.L., Kriel, H., Ramsey, J., Randy Bryant, R., Elliot, L., Fowler, J., Landiau, M., Leck, R., Odewahn, S., Perry, D., Savage, R., Schroeder Mrozinski, E., Shetrone, M., Damm, G., Gebhardt, K., MacQueen, P.J., Martin, J., Armandroff, T., Ramsey, L.W., "The Hobby-Eberly Telescope wide-field upgrade", Proc. SPIE 9906-5 (2016)

[7] Buckley, D.A.H., Swart, G.P., Meiring, J.G., "Completion of the Southern African Large Telescope", *Proc. SPIE*, 6267-19 (2006)

[8] Hill, G.J., MacQueen, P.J., Smith, M.P., Tufts, J.R., Roth, M.M., Kelz, A., Adams, J.J., Drory, N., Barnes, S.I., Blanc, G.A., Murphy, J.D., Gebhardt, K., Altmann, W., Wesley, G.L., Segura, P.R., Good, J.M., Booth, J.A., Bauer, S.-M., Goertz, J.A., Edmonston, R.D., Wilkinson, C.P., "Design, construction, and performance of VIRUS-P: the prototype of a highly replicated integral-field spectrograph for HET", *Proc. SPIE*, 7014-257 (2008)

[9] Hill, G.J., Tuttle, S.E., Vattiat, B.L., Lee, H., Drory, N., Kelz, A., Ramsey, J., DePoy, D.L., Marshall, J.L., Gebhardt, K., Chonis, T.S., Dalton, G.B., Farrow, D., Good, J.M., Haynes, D.M., Indahl, B.L., Jahn, T., Kriel, H., Montesano, F., Nicklas, H., Noyola, E., Prochaska, T., Allen, R.D., Blanc, G., Fabricius, M.H., Landriau, M., MacQueen, P.J., Roth, M.M., Savage, R., Snigula, J.M., "VIRUS: first deployment of the massively replicated fiber integral field spectrograph for the upgraded Hobby-Eberly Telescope", Proc. SPIE, 9908-54 (2016)

[10] Hill, G.J., Kelz, A., Lee, H., MacQueen, P.J., Peterson, T., Ramsey, J., Vattiat, B.L., DePoy, D.L., Drory, N., Gebhardt, K., Good, J.M., Jahn, T., Kriel, H., Marshall, J.L., Montesano, F., Tuttle, S.E., Balderrama, E., Chonis, T.S., Dalton, G.B., Fabricius, M.H., Farrow, D., Fowler, J.R., Froning, C., Haynes, D.M., Indahl, B.L., Martin, J., Montesano, F., Mrozinski, E., Nicklas, H., Noyola, E., Odewahn, S., Peterson, A., Prochaska, T., Shetrone, M., Smith, G., Snigula, J.M., Spencer, R., Zeimann, G., "VIRUS: status and performance of the massively replicated fiber integral field spectrograph for the upgraded Hobby-Eberly telescope", Proc. SPIE, 10702-56 (2018)

[11] Kelz, A., Jahn, T., Haynes, D.M., Hill, G.J., Murphy, J.D., Rutowska, M., Streicher, O., Neumann, J., Nicklas, N., Sandin, C., Fabricius, M., "HETDEX / VIRUS: testing and performance of 33,000 optical fibres", Proc. SPIE, 9147-269 (2014)

[12] Vattiat, B.L., Hill, G.J., Kelz, A., Martin, J., Mrozinski, E., Jahn, T., Spencer, R., "Deployment and handling of the VIRUS fiber integral field units", 10702-303 (2018)

[13] Prochaska, T., Allen, R., Rheault, J. P., Cook, E., Baker, D., DePoy, D. L., Marshall, J. L., Hill, G., Perry, D., "VIRUS instrument enclosures," Proc. SPIE 9147-257 (2014)
[14] Smith, M.P., Mulholland, G.T., Booth, J.A., Good, J.M., Hill, G.J., MacQueen, P.J., Rafal, M.D., Savage, R.D., Vattiat, B.L., "The cryogenic system for the VIRUS array of spectrographs on the Hobby Eberly Telescope", Proc. SPIE, 7018-117 (2008)
[15] Chonis, T.S., et al., "Development of a cryogenic system for the VIRUS array of 150 spectrographs for the Hobby-Eberly Telescope," Proc. SPIE, 7735-265 (2010)
[16] Spencer, R., Balderrama, E., Damm, G., Fowler, J., Good, J., Hill, G.J., Kriel, H., MacQueen, P.J., Mrozinski, E., Perry, D., Peterson, T., Shetrone, M., Savage, R., Cook, E., Smith, G., DePoy, D.L., Marshall, J.M., Prochaska, T., Sauceda, M., "VIRUS: the instrument infrastructure to support the deployment and upkeep of 156 spectrographs at the Hobby-Eberly telescope", 10706-246 (2018)
[17] Lee, H., Vattiat, B.L., Hill, G.J., "Efficient high-precision CCD-field lens alignment and integration process of mass-produced fast astronomical spectrograph cameras with VIRUS as an example", 10706-55 (2018)
[18] Hill, G.J., "HETDEX and VIRUS: Panoramic Integral Field Spectroscopy with 35k fibres" in 'Multi-Object Spectroscopy in the Next Decade' a conference held in La Palma, March 2015, (eds. I. Skillen, M. Balcells & S. Trager), ASP Conference Series, 507, 393 (2016)
[19] Hill, G.J., Gebhardt, K., Komatsu, E., Drory, N., MacQueen, P.J., Adams, J.A., Blanc, G.A., Koehler, R., Rafal, Roth, M.M., Kelz, A., Grupp, F., Murphy, J., Palunas, P., Gronwall, C., Ciardullo, R., Bender, R., Hopp, U., and Schneider, D.P., "The Hobby-Eberly Telescope Dark Energy Experiment (HETDEX): Description and Early Pilot Survey Results", in Panoramic Views of the Universe, ASP Conf. Series, 399, 115 (2008)
[20] Burge, J.H., Benjamin, S.D., Dubin, M.B., Manuel, S.M., Novak, M.J. Oh, C.J., Valente, M.J., Zhao, C., Booth, J.A., Good, J.M., Hill, G.J., Lee, H., MacQueen, P.J., Rafal, M.D., Savage, R.D., Smith, M.P., Vattiat, B.L., "Development of a wide-field spherical aberration corrector for the Hobby Eberly Telescope", Proc. SPIE, 7733-51 (2010)
[21] Oh, C.-J., Frater, E., Zhao, C., Burge, J.H., "System alignment and performance test of a wide field corrector for the Hobby-Eberly telescope", Proc. SPIE, 9145-8 (2014)
[22] Lee, H., Hill, G.J., Good, J.M., Vattiat, B.L., Shetrone, M., Martin, J., Schroeder Mrozinski, E., Kriel, H., Oh, C.-J., Frater, E., Smith, B., Burge, J.H., "Delivery, installation, on-sky verification of Hobby Eberly Telescope wide-field corrector," Proc. SPIE 9906-156 (2016)
[23] Good, J.M., Lee, H., Hill, G.J., Vattiat, B.L., Perry, D., Kriel, H., Savage, R., "Design and Implementation of Coating Hardware for the Hobby-Eberly Telescope Wide Field Corrector", Proc. SPIE, 9145-160 (2014)
[24] Good, J.M., Hill, G.J., Schroeder-Mrozinski, E., Savage, R., Kriel, Benjamin, H.S., Stone, R., "Performance of Cable Isolators in the Transport of Large Optical Assemblies", Proc. SPIE 9906-14 (2016)
[25] Mollison, N.T., et al., "Design and development of a long-travel positioning actuator and tandem constant force actuator safety system for the Hobby-Eberly Telescope wide field upgrade," Proc. SPIE, 7733-150 (2010)
[26] Zierer, Jr., J.J., Wedeking, G.A., Beno, J.H., Good, J.M., "Design, testing, and installation of a high-precision hexapod for the Hobby-Eberly Telescope dark energy experiment (HETDEX)," Proc. SPIE, 8444-176 (2012)
[27] Worthington, M.S., et al., "Design and development of a high-precision, high-payload telescope dual-drive system," Proc. SPIE, 7733-201 (2010)
[28] Soukup I.M., et al., "Testing, characterization, and control of a multi-axis, high precision drive system for the Hobby-Eberly Telescope Wide Field Upgrade," Proc. SPIE, 8444-147 (2012)
[29] Good, J.M., Hill, G.J., Leck, R.L., Landriau, M., Drory, N., Fowler, J.R., Kriel, H., Cornell, M.E., Booth, J.A., Lee, H., Savage, R., "Laboratory Performance Testing, Installation, and Commissioning of the Wide Field Upgrade Tracker for the Hobby-Eberly Telescope", Proc. SPIE, 9145-156 (2014)
[30] Good, J.M., Hill, G.J., Landriau, M., Lee, H., Schroeder-Mrozinski, E., Martin, J., Kriel, H., Shetrone, M., Fowler, J., Savage, R., Leck, R., "HET Wide Field Upgrade Tracker System Performance", Proc. SPIE 9906-167 (2016)
[31] Good, J.M., Leck, R., Ramsey, J., Drory, N., Hill, G.J., Fowler, J.R., Kriel, H., Landriau, M., "Mechanical systems performance of the HET wide-field upgrade", 10700-143 (2018)
[32] Vattiat, B.L., et al., "Design, testing, and performance of the Hobby Eberly Telescope prime focus instrument package," Proc. SPIE, 8446-269 (2012)
[33] Vattiat, B.L., Hill, G.J., Lee, H., Moreira, W., Drory, N., Ramsey, J., Elliot, L., Landriau, M., Perry, D.M., Savage, R., Kriel, H., Haeuser, M., Mangold, F., "Design, alignment, and deployment of the Hobby Eberly Telescope prime focus instrument package", Proc. SPIE, 9147-172 (2014)

[34] Lee, H., et al., “Analysis of active alignment control of the Hobby-Eberly Telescope wide field corrector using Shack-Hartmann wavefront sensors,” Proc. SPIE, 7738-18 (2010)
[35] Lee, H., et al., “Metrology systems for the active alignment control of the Hobby-Eberly Telescope wide-field upgrade,” Proc. SPIE, 7739-28 (2010)
[36] Lee, H., et al., “Metrology systems of Hobby-Eberly Telescope wide field upgrade,” Proc. SPIE, 8444-181 (2012)
[37] Lee, H., Hill, G.J., Drory, N., Ramsey, J., Bryant, R., Shetrone, M., “Wavefront sensing for active alignment control of a telescope with dynamically varying pupil geometry: theory, implementation, on-sky performance”, Proc. SPIE, 10706-150 (2018)
[38] Lee, H., Hill, G.J., Drory, N., Vattiat, B.L., Ramsey, J., Bryant, R., Shetrone, M., Odewahn, S., Rostopchin, S., Landriau, M., Fowler, J., Leck, R., Kriel, H., Damm, G., “New Hobby Eberly telescope metrology systems: design, implementation, and on-sky performance”, 10700-78 (2018)
[39] Beno, J.H., *et al*., “HETDEX tracker control system design and implementation,” Proc. SPIE, **8444**-211 (2012)
[40] Ramsey, J., Drory, N., Bryant, R., Elliott, L., Fowler, J., Hill, G. J., Landriau, M., Leck, R., Vattiat, B., "A control system framework for the Hobby-Eberly Telescope", Proc. SPIE, 9913-160 (2016)
[41] Ramsey, J., Bryant, R., Drory, N., Elliott, L., Fowler, J., Good, J., Hill, G.J., Landriau, M., Lee, H., Leck, R., Kolbly, L., Vattiat, B.L., “Simulation strategies employed in the development and maintenance of the Hobby-Eberly telescope control system”, 10707-117 (2018)
[42] Wolf, M.J., Palunas, P., Booth, J.A., Ward, M.H., Wirth, A., Wesley, G.L., O’Donoghue, D., Ramsey, L.W., “Mirror Alignment Recovery System (MARS) on the Hobby-Eberly Telescope,” Proc. SPIE, 4837 Large Ground Based Telescopes (2003)
[43] Lee, H., Hill, G.J., Vattiat, B.L., Smith, M.P., Haeuser, M., “Facility calibration unit of Hobby Eberly Telescope wide field upgrade,” Proc. SPIE, 8444-172 (2012)
[44] Adams, M.T., Palunas, P., Booth, J.A., Fowler, J.R., Wolf, M.J., Ames, G.A., Rakoczy, J.M., Montgomery, E.E., "Hobby-Eberly Telescope Segment Alignment Maintenance System," Proc. SPIE 4837, Large Ground-based Telescopes (2003)
[45] Chonis, T.S., Hill, G.J., Lee, H., Tuttle, S.E., Vattiat, B.L., Drory, N., Indahl, B.L., Peterson, T.W., Ramsey, J., “LRS2 – design, assembly, testing, and commissioning of the second generation low resolution spectrograph for the Hobby-Eberly Telescope”, Proc. SPIE 9908-163 (2016)
[46] Mahadevan, S., Anderson, T., Bender, C., Halverson, S., Hearty, F., Levi, E., YLi, Y., Monson, A., Nelson, M., Ramsey, L., Robertson, P., Roy, A., Schwab, C., Kári Stefánsson, G., Terrien, R., “The habitable-zone planet finder: AI&V status and summary of research and development to achieve high precision NIR Doppler radial velocities”, Proc SPIE, 9908-40 (2016)
[47] Mahadevan, S., et al, “The habitable-zone planet finder: engineering and commissioning on the Hobby Eberly telescope,” Proc. SPIE 10702-40 (2018)
[48] Tull, R.G., “High-resolution fiber-coupled spectrograph of the Hbby-Eberly Telescope,” Proc. SPIE, 3355, Optical Astronomical Instrumentation (1998)
[49] MacQueen, P.J., South, B.J., Strubhar, J.L., Wesley, G.L., Odoms, P.S. Edmonston, R.D., “The Hobby Eberly Telescope high resolution spectrograph upgrade”, Proc. SPIE, 9908-42 (2016)
[50] Hill, G. J., Nicklas, H., MacQueen, P. J., Tejada de V., C., Cobos D., F. J., and Mitsch, W., "The Hobby-Eberly Telescope Low Resolution Spectrograph", Proc. SPIE, Optical Astronomical Instrumentation 3355 (1998)